Nanotechnology Perceptions
ISSN 1660-6795
www.nano-ntp.com

Design and Simulation of a Hybrid Wind-Photovoltaic System for Energy Supply

Diego Farez, Erick Chicaiza, Diego L. Jiménez, Roberto Salazar A.

Facultad de Ciencias de la Ingeniería y Aplicadas, Universidad Técnica de Cotopaxi, Latacunga, Ecuador
Email: diego.farez5642@utc.edu.ec

This document consists of the design and simulation of a hybrid wind-photovoltaic system to implement a prototype that can be used to charge electronic equipment. Through the use of non-conventional renewable energy without connection to the electrical grid. Due to the need presented by public transport users in rural areas. For which a meteorological study is carried out to size the system based on the behavior of the data on wind speed and solar radiation for one month under real measurements, and extrapolating the data to one year from the Method of Monte Carlo. Likewise, by estimating the electrical load and based on the technical characteristics of the elements available on the market, a design for the hybrid wind-photovoltaic system is proposed. Then a simulation of the prototype is carried out in the Simulink software, integrating all the elements of the system, and through the use of the characteristic equations of the solar panels, as well as the wind turbine, the validation of the operation of the prototype is carried out. Finally, it is possible to verify that when the battery is 100% charged, the system produces 120 VAC and 378 W of enough power to supply the proposed demand of 200 W, achieving a functional and efficient design for its future implementation.
Keywords: Hybrid system, solar generation, wind generation, design, simulation.

1. Introduction

Energy sourcing through non-conventional renewable energy (NCRE) sources presents a significant challenge due to the need to consider random variables such as wind speed and solar radiation. Currently, most industrialized countries are turning to renewable-based power generation systems with integrated energy storage systems. This is due to the high costs associated with the generation, transmission, and distribution of electricity, as well as

the pollution generated by the use of fossil fuels [1].

NCRE-based energy resources emerge as an innovative and beneficial solution in the fight against climate change and the promotion of equitable access to electricity. These resources, which include solar, wind, biomass, among others, are increasingly being adopted around the world [2]. Their implementation contributes to reducing greenhouse gas emissions, and also allows energy to be brought to isolated places and economically disadvantaged communities. In this sense, NCRE resources are an environmentally sustainable solution, as they emerge as the key driver for inclusive development and the alleviation of energy poverty at the global level [3].

With time and advances in research, it has been possible to combine various NCRE sources to meet specific demands, giving rise to hybrid generation systems. These systems have become an efficient alternative for electrifying rural areas. While countries such as Italy, Spain, China and others have implemented various systems to supply electronic devices in urban areas and public spaces, promoting energy development independent of the traditional electricity grid. This ranges from charging devices such as cell phones, wireless speakers to electric bicycles [4].

A hybrid non-conventional renewable energy system consists of the combination of two or more energy sources to optimize the efficiency of each technology. For example, on windy and cloudy days, wind turbines are more efficient, while on clear days solar energy is more usable. This combination maximizes the environmental conditions for the generation of electrical power [5]. Therefore, the implementation of a hybrid system makes it possible to optimize its design, predict its performance, analyze its efficiency and robustness, reduce costs and risks, and contribute to technological progress in the NCRE sector [6].

Below is a state-of-the-art that explores the current research landscape on the Design and Simulation of Hybrid Wind-Photovoltaic Systems for Energy Supply.

In [7] a document is presented that analyzes the potential of photovoltaic solar energy in Ecuador and the government's efforts to promote its use, with the aim of achieving a 15% share of non-conventional renewable energy in the energy matrix by 2030. Concluding that photovoltaic solar energy has great potential in Ecuador and can contribute significantly to the country's energy transition. Likewise, [8] talks about the advantages offered by the use of non-conventional renewable energies, especially in rural or mountainous areas, where natural resources are a considerable advantage. Territorial strategy based on the evaluation of natural sources such as solar radiation and wind speed can be highly beneficial for local and regional development.

On the other hand, in [9], a comparison is made between mathematical modeling and the simulation of a solar panel in Simulink software, in order to identify the best method to characterize the energy potential. The power generated under various conditions is used, and the two methods are compared using real solar radiation and panel operating temperature data. It is concluded that both techniques have a good correlation, although the mathematical model offers a better approximation. While in [10] the Monte Carlo Method is employed to create synthetic series by generating multiple possible scenarios based on probability distributions, and thus evaluate the health status of lithium-ion batteries under different usage

scenarios in the context of microgrids and electric vehicles.

For all of the above, it can be concluded that, in the Ecuadorian context, the amount of solar and wind resources stands out due to the country's privileged location on the globe, therefore the need arises to create a mixed system that allows the use of solar energy through photovoltaic cells and wind energy through wind turbines. to supply the demand of places isolated from the electricity grid such as bus stops, parks, study centers, among others. Where the population has the need to charge electronic devices of all kinds while carrying out their daily activities, avoiding additional costs for portable chargers and motivating the use of NCRE.

Finally, this document proposes the design and simulation of a hybrid wind-photovoltaic system in order to supply electronic devices in rural areas, using non-conventional renewable energy sources such as solar and wind, and allowing the creation of autonomous charging centers for the user of public transport and students from different educational centers. so that they can charge their mobile devices while carrying out their daily activities, and promoting the use of clean energy that does not cause harm to the environment.

2. DEVELOPMENT

The methodology for the development of the project consists of three main stages. First, the solar and wind resources available in the selected location are evaluated, with the aim of determining the energy potential necessary for the operation of the system. In the second stage, the hybrid wind-photovoltaic system is designed, based on the analysis of the project's loads and the sizing of the equipment required for its future implementation. Finally, the hybrid system is simulated using Simulink software. During this stage, a model of the system is built using the previously dimensioned elements, and its operation is evaluated with the input data corresponding to the solar and wind resource of the analyzed location.

2.1 Solar and Wind Resource Assessment

The evaluation of the solar and wind resource is carried out in the San Juan neighborhood, Latacunga canton, Cotopaxi province, under the geographical coordinates: -0.9547882418655281, -78.62924120601562. Fig. 1 shows the exact location intended for the development of the project. The measurement instruments used for data acquisition are specified in Table 1. For which the technical characteristics of the Apogee MP-200 pyranometer are obtained from [11], while the datasheet of the Acurite proffesional weather center anemometer is obtained from [12].

Figure 1: Location of the solar and wind resource measurement

Table 1: Technical characteristics of the measuring instruments

MP-200 Pyranometer	
Specification	Detail
Calibration uncertainty at 1000 W/m²	Less than 3%
Non-linearity	Less than 1% up to 2000 W/m²
Response Time	Less than 1 ms
Field of view	180°

MP-200 Pyranometer	
Specification	Detail
Calibration uncertainty at 1000 W/m²	Less than 3%
Non-linearity	Less than 1% up to 2000 W/m²
Response Time	Less than 1 ms
Field of view	180°
Spectral Range	360 to 1120 nm
Sensor dimensions	Integrated with gauge: 24 mm diameter, 33 mm height
Meter Dimensions	126 cm long, 70 mm wide, 24 mm high
Acurite Proffesional Weather Center Anemometer	
Specification	Detail
Wind Speed	0 to 99 mph; 0 to 159 kph
Wind Speed Accuracy	+/- 2 mph below 10 mph +/- 3 mph from 10 to 30 mph +/- 4 mph from 30 to 50 mph +/- 5 mph from 50 to 99 mph
Wireless Range	330 feet / 100 meters depending on the home's building materials

Data Update	Wind Speed: Updates every 18 seconds<br
Dimensions	8.2 inches high x 6.7 inches wide x 2.7 inches deep

With the data obtained by the pyranometer, the analysis of solar radiation can be carried out as shown in Fig. 2, where the behavior of the irradiation of each day of the month of February 2024 is observed. Solar radiation can be identified as being present from 6:00 a.m. to 6:00 p.m. Approximately 5 hours as peak solar time. It is also observed that the 23rd of the month presents the highest solar radiation at 12:00 with a value of , on the other hand it is observed that the 4th of the month presents the lowest solar radiation at 12:00 registering a value of . This shows that the solar resource is sufficient for the proper functioning of the photovoltaic modules.620 W/m^2 200 W/m^2

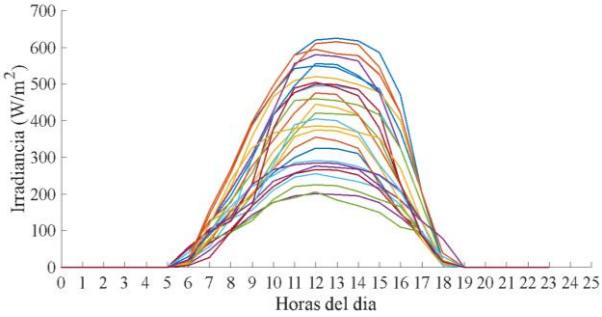

Figure 2: Solar resource measurement

With the data obtained by the anemometer, the analysis of the wind resource can be carried out as shown in Fig. 3, where the behavior of the wind speed during the month of February 2024 is observed. In addition, it can be identified that the greatest variation in wind speed is located from 8:00 a.m. to 5:00 p.m. It is also observed that the 7th of the month has the highest wind speed of 1:00 p.m., while the 27th of the month registers the lowest wind speed with a value of 1:00 p.m. This shows that even though the wind resource is very variable throughout the day, the wind speed is sufficient for the operation of a wind turbine with a vertical axis.6,49 m/s0,39 m/s

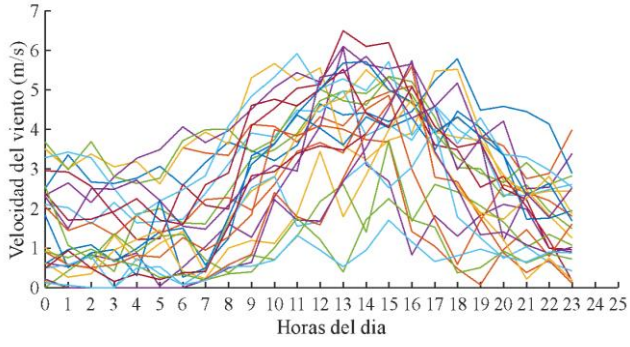

Figure 3: Wind resource measurement

As we have measurements only from the month of February 2024 for both wind and solar resources, synthetic series are generated using the Monte Carlo Method based on the work presented in [10]. In this way, it is possible to extrapolate the data to obtain wind speed and solar radiation values for the entire year 2024. Because the synthetic series keep the characteristics of the original series, and by using a normal probability distribution for solar radiation and Weibull probability distribution for wind speed, it is possible to generate random scenarios including the variability of the resource and therefore obtaining results closer to reality.

Fig. 4 shows the response of the Monte Carlo Method for solar radiation, where 10 curves can be evidenced that represent the average irradiance of the months of March to December 2024, in this way the behavior similar to the data measured from February 2024 can be observed. where there is a range of A of monthly solar radiation at 12:00 noon, maintaining approximately 5 hours of peak solar time, a sufficient value for the proper operation of the photovoltaic modules. $\mathbf{403\ W/m^2 432\ W/m^2}$

Likewise, Fig. 5 shows the response of the Monte Carlo Method for wind speed, where 10 average wind speed curves projected for the months of March to December 2024 can be evidenced, in this way the behavior similar to the data measured from February 2024 can be observed. In addition, there is evidence of an average variation of the wind resource of a during the 24 hours of the day. In this sense, it is important to locate a wind turbine with a vertical axis that can operate with low wind speed values, and thus achieve greater electrical power from the wind resource for the operation of the hybrid system.$\mathbf{1,38\ m/s4,51\ m/s}$

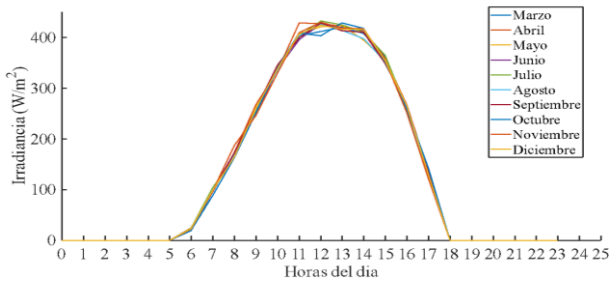

Figure 4: Projection of average solar radiation for the months of March to December 2024

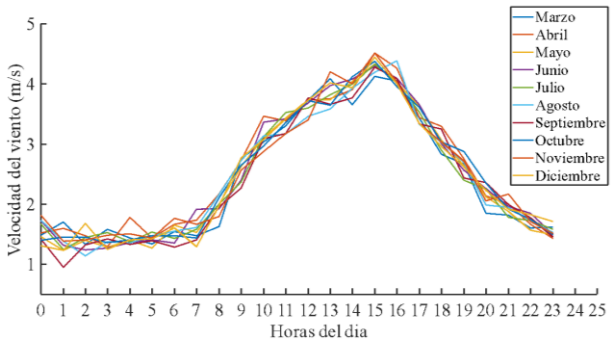

Figure 5: Projection of the average wind speed for the months of March to December 2024

2.2 Hybrid System Design

To carry out the design of the hybrid system, it begins with the creation of a scheme of the elements that will be used within the project. Subsequently, a load study is carried out to ensure an adequate sizing of the system. The elements of the photovoltaic system must comply with the IEC-61215 or IEEE-1262 standard, likewise the charge controllers must be turned off to the UL 1741 standard or other applicable standards as detailed in [13]. This will make it possible to identify suitable components for the operation of the hybrid system, and that are available in the Ecuadorian market for future implementation.

Fig. 6 shows the diagram of the hybrid wind-photovoltaic system, where the elements proposed to carry out the design of the project can be evidenced, identifying that the system is composed of several stages such as: solar and/or wind energy generation, energy conversion and investment, and hybrid energy storage through batteries to supply demand.

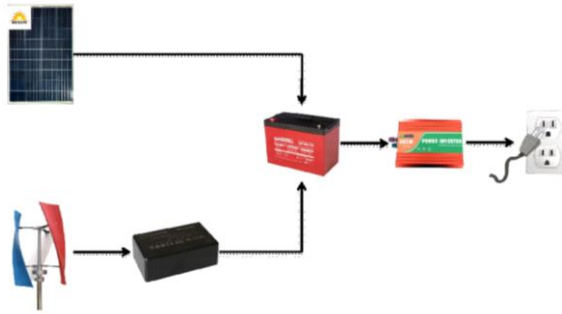

Figure 6: Diagram of the hybrid wind-photovoltaic system

To carry out the sizing of the hybrid system, the lifting of loads is carried out as shown in Table 2, taking as a reference the values established in [14], 1 double outlet and a USB outlet of 200W each are located, making 5 hours of use for each element, and a demand factor of 0.5 a total daily energy of , In this way, the load that must be supplied for the hybrid system is proposed. Subsequently, the equipment that will be used for the design of the hybrid system is dimensioned according to the established demand, as shown in Table 3. Where the powers and currents necessary for the correct operation of the system are presented. $\mathbf{2000}\,\boldsymbol{Wh/día}$

Table 2: Hybrid System Demand

Team	#	Rated Power (W)	Hours of use per day (H)	Demand Factor	Energy per day (Wh/day)
Dual power outlet	1	200	5	0,5	1000
USB power outlet	1	200	5	0.5	1000
TOTAL	2	400	10	0.5	2000

Table 3: Hybrid System Sizing

Magnitude	Valu e	Unit
Daily Energy	2000	$\boldsymbol{Wh/día}$
Total power with utilization factor of $\mathbf{0.5}$	200	$\boldsymbol{W}$
System Voltage	120	$\boldsymbol{V}$
Current Time	1.67	$\boldsymbol{Ah}$
Current per day	16.67	$\boldsymbol{Ah/día}$

Table 4 shows the technical characteristics of the photovoltaic panels and the wind turbine selected from the sizing of the demand for the hybrid system and the corresponding regulations, as well as identifying that they are available in the Ecuadorian market and have an affordable price for a future implementation of the project.

Table 4: Technical characteristics of photovoltaic panels and wind turbine

Photovoltaic Panel	
Power:	$\mathbf{110}\,\boldsymbol{W}$
Rated Voltage:	12 VDC
Dimensions:	$\mathbf{1120}\,\boldsymbol{x}\,\mathbf{670}\,\boldsymbol{x}\,\mathbf{30}\,\boldsymbol{mm}$
Weight: 8.4 kg	$\mathbf{8.4}\,\boldsymbol{Kg}$
Wind turbine	
Rated Power	$>\mathbf{300}\,\boldsymbol{W}$
Nominal voltage	$\mathbf{96}\,\boldsymbol{V}-\mathbf{220}\,\boldsymbol{V}$
Rotor diameter	$\mathbf{530}\,\boldsymbol{mm}$
Weight	$\mathbf{14}\,\boldsymbol{Kg}$

On the other hand, the inverter must be able to withstand temporary load peaks, which are usually higher than the rated load, an input voltage of and an output of , this voltage depending on the storage system of a battery of y . In this context it is possible to calculate the discharge capacity of the battery from [15], as shown in equation (1). $\mathbf{12}\,\boldsymbol{VDC}\mathbf{100}-\mathbf{120}\,\boldsymbol{VAC}\mathbf{12}\,\boldsymbol{VDC}\mathbf{100}\,\boldsymbol{AhC_{DB}}$

$$\boldsymbol{C_{DB}} = \frac{\boldsymbol{V_B} * \boldsymbol{I_B}}{\boldsymbol{V_B} * \boldsymbol{I_{consumida}}} * \boldsymbol{P_{desc}} \qquad (1)$$

Where is the battery voltage, is the battery current in , is the current consumed per hour of the battery as specified in Table 3, and is the depth of discharge of the battery. Whereas, to calculate the battery's charge capacity, equation (2) is used. $\boldsymbol{V_B I_B Ah I_{consumida} P_{desc}}$

$$\boldsymbol{C_{CB}} = \frac{\boldsymbol{C_B} * \boldsymbol{EFIC}}{\boldsymbol{I_{CT}} - \boldsymbol{I_{consumida}}} \qquad (2)$$

Where is the battery charge capacity, is the battery capacity in , is the battery efficiency, and is the total charge current. To obtain this current, equation (3) is used. $\boldsymbol{C_{CB} C_B Ah EFIC I_{CT}}$

$$I_{CT} = I_{CS} + I_{CE} \quad (3)$$

Where is the solar charging current and is the wind charging current. $I_{Cs} I_{CE}$

Table 5 shows the technical characteristics that the battery must have based on the calculations made. Highlighting a charging time of approximately 21.62 hours, which corresponds to a high energy absorption capacity of the battery in a relatively short period of time. Also, a discharge time of approximately 60 hours, which means that the energy storage system has a high energy retention capacity, and can provide significant energy autonomy to the hybrid system under study.

Table 5: Technical characteristics of the battery

Magnitude	Value	Unit
Battery capacity	**100**	***Ah***
Efficiency	**90**	(%)
Voltage of the 2 panels	**24**	***V***
Solar charging current	**5,75**	***A***
Wind load current	**0,08**	***A***
Total Load Current	**5,83**	***A***
Battery power	**1200**	***Wh***
Current consumption	**1.67**	***A***
Charging Time	**21.62**	***horas***
Download Time	**60**	***horas***

To guarantee a system with daily power of , a total power of and an input voltage of , the inverter must have an overload factor of to maintain an adequate safety margin, i.e. an inverter of at least power with an efficiency greater than . This sizing ensures that the inverter can handle continuous loads and peaks efficiently and reliably. Also, taking into account an hourly power consumption of , it is necessary to select a protection of ensuring a safety margin of the according [15]. This protective device will ensure that the system is protected against overcurrents, while allowing for normal, uninterrupted operation of the hybrid system.2000 Wh200 W12 VDC1.5300 W90 %1.67 A20 A125 %

Once the elements of the project have been selected, the design of the hybrid system is presented through Fig. 7, where the structure made up of photovoltaic panels, a vertical axis wind turbine and a load center is shown, in this way all this set of elements are placed on a 3-meter-high pole. For which the wind turbine is placed in the middle-upper part of the structure to obtain its highest efficiency, while the solar panels are located on the sides of the turbine with an inclination of 15° for maintenance purposes, therefore in the load center that is inside the structure is included the DC/AC inverter systems, storage and protection. Regarding the outlets, they are arranged at the bottom of the pole for the user to use.

Finally, in Fig. 8, the electrical diagram of the hybrid system is shown where the connections that must be made to carry out the correct operation of the project are observed, it should be noted that the solar panels have polarity as they are direct current outputs, in that sense the

red color has been defined as positive and the blue color negative, Likewise, for the output of the inverter to the load, there is alternating current, so phase and neutral have been defined, represented by the color red and blue, respectively.

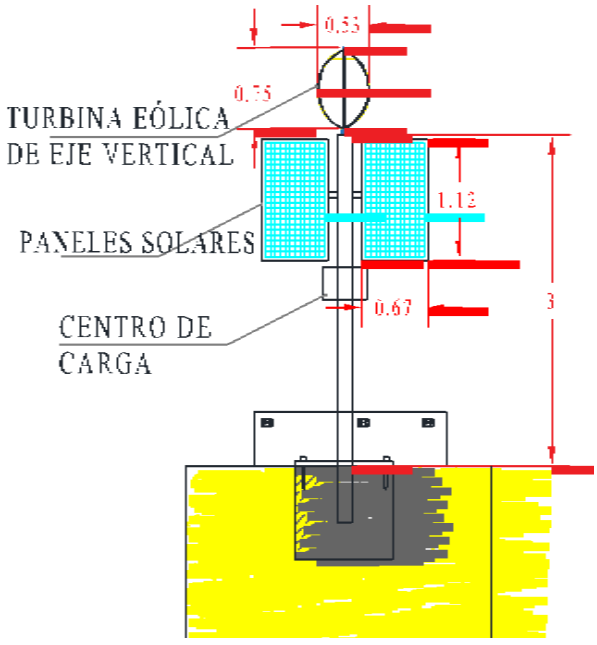

Figure 7: Hybrid System Design

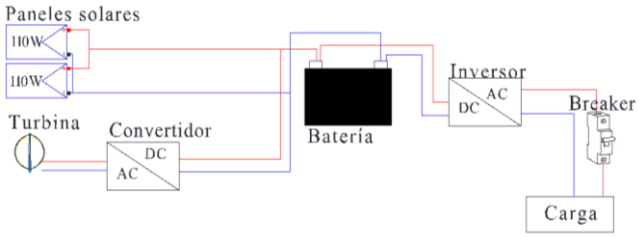

Figure 8: Electrical diagram of the hybrid system

2.3 Hybrid System Simulation

The simulation of the hybrid wind-photovoltaic system is carried out in Matlab's Simulink software as shown in the diagram in Fig. 9, where the use of a photovoltaic module, a wind turbine, an AC/DC converter, a battery, a DC/AC inverter and a load can be identified, in this way the operation of the hybrid system is simulated based on the following characteristics:

The input of the photovoltaic panels uses an average monthly irradiance of from the estimates carried out in section 2.1., considering a constant temperature of since integrated temperature control is assumed. A wind speed value of based on the estimates in section 2.1. is also placed as input to the wind turbine, in addition, a beta angle of . This value

corresponds to the greater efficiency that the wind turbine can deliver since it establishes a Betz limit of , which is within its maximum operating range and thus guarantees the best efficiency of the wind turbine.432 W/m^2 25 °C4,51 m/s0°Cp=0,41

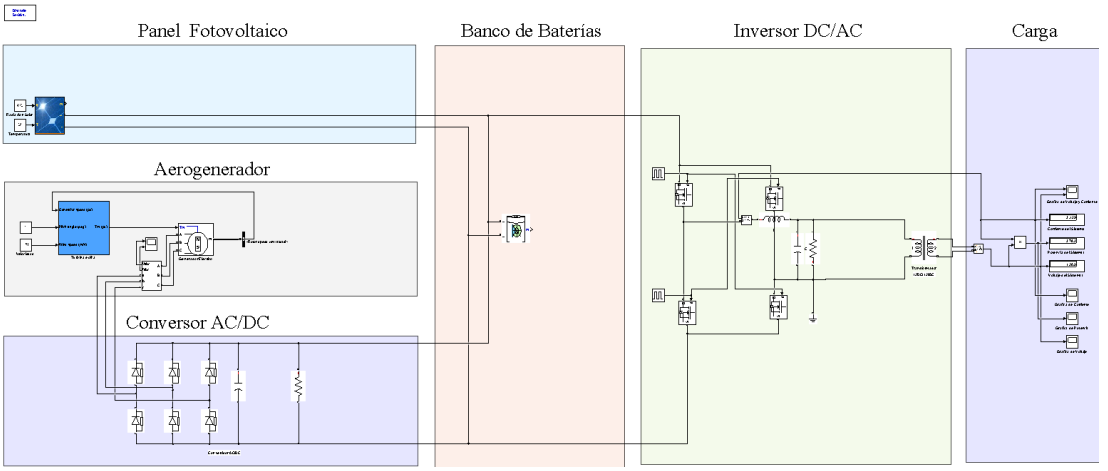

Figure 9: Hybrid System Simulation Performed in Simulink

The output of the photovoltaic panels has voltage and current in DC, while the output of the wind turbine has voltage and current in AC, so an AC/DC converter coupled to the wind turbine is necessary in order to have a DC bus composed of the panels and the wind turbine. The DC bus output is connected to the battery bank in parallel, so the solar and wind resource charges the battery bank. Now, because the loads are in AC, it is necessary to use a DC/AC inverter, which allows obtaining the voltage, current and power parameters that the load needs to be supplied. In this case, the following outputs are obtained: a voltage of , a current of and a power of being sufficient parameters to supply the proposed load of .120 VAC3,13 A378 W200 W

The characteristics of each element within the simulation are presented below, in such a way that the model of the photovoltaic modules is established in Fig. 10, where the power output depends on the input data corresponding to solar radiation and temperature. In this way, to obtain the nominal power of the two panels, it is used as an input for temperature and solar radiation, obtaining as a voltage of 25 °C1000 W/m^2 178,92 V, a current of , and a power of . 1,23 A220,1 W

Whereas, for our particular case, a solar radiation value of has been established 432 W/m^2 from the evaluation of solar resource in section 2.1., and considered a temperature control to which the25°C following results can be obtained: a voltage of 192,9 V, a current of , and a power of , identifying that as solar radiation is reduced, the power of the panel is also reduced, so it can be defined that these values are directly proportional, as can be seen in the maximum power curves of the 2 proposal panels in Fig. 11.0,54 A105,9 W110 W

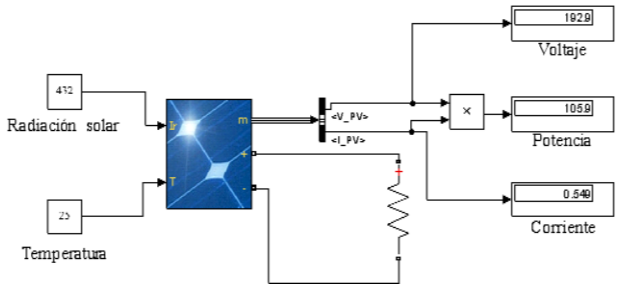

Figure 10: PV Panel Model in Simulink

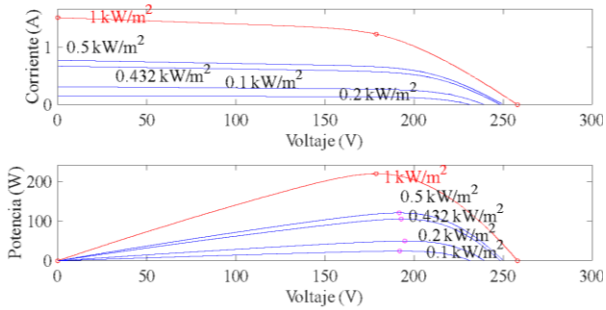

Figure 11: Maximum power curves for two 110 W panels

From [16] it is possible to represent the equations that govern the photovoltaic panel, so to find the output power equation (4) is used, considering that the temperature remains constant and the parameter that varies is only solar radiation.

$$P_{m(G_m)} = FF * V_{oc(G_m)} * I_{sc(G_m)} \qquad (4)$$

Where, , is the panel form factor, , is the open circuit voltage at an irradiance level, $FFV_{oc(G_m)}I_{sc(G_m)}$, is the short-circuit current at an irradiance level. To find the value of the when varying solar radiation, equation (5) is used.$V_{oc(G_m)}$

$$V_{oc(G_m)} = V_{oc(nom)} + \frac{n * k_b * T}{q} ln\left(\frac{G_m}{G_{nom}}\right) \qquad (5)$$

Where, , is the nominal open-circuit voltage of the panel, , is the ideality factor of the panel, , is the Boltzmann constant of (), is the electron charge of (), , is irrandiance under standard measurement conditions of () and , is the irrandiance impinging on the photovoltaic module. Therefore, it is necessary to find the value of the short-circuit current for which equation (6) is used.$V_{oc(nom)}nk_b1.381 \cdot 10^{-23}\,J/Kq1.602 \cdot 10^{-19}\,CG_{nom}1000\,W/m^2G_mI_{sc(G_m)}$

$$I_{sc(G_m)} = I_{nom} * \frac{G_m}{G_{nom}} \qquad (6)$$

Where, , is the nominal current of the PV module. To determine the form factor of the

photovoltaic panel, it is done using equation (7).$\boldsymbol{I_{nom}FF}$

$$\boldsymbol{FF = \frac{P_{nom}}{V_{oc(G_m)} * I_{sc(G_m)}}} \qquad (7)$$

Where, , is the nominal power of the photovoltaic panel. Another important aspect is the internal resistance of the photovoltaic panel which is obtained from equation (8), where , is the nominal maximum voltage of the panel.$\boldsymbol{P_{nom}V_{max}}$

$$\boldsymbol{R = \frac{{P_{nom}}^2}{V_{max}}} \qquad (8)$$

On the other hand, the wind turbine model is presented in Fig. 12, where the power output depends on the input data of the wind speed and the beta angle. Thus, to obtain the nominal power of the turbine, a wind speed of , and a beta angle of , are used, obtaining as output a power of is . Whereas, for this particular case, the average wind speed values set out in section 2.1., and an angle where$\boldsymbol{11\ m/s0°3000\ W4,51\ m/s\beta = 0°}$ a power output of . $\boldsymbol{277,22\ W}$In Fig. 13 you can identify the characteristic curves of the wind turbine, showing that it can generate power with low wind speed values for different operating curves.

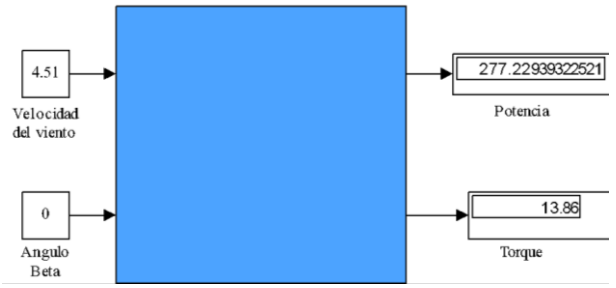

Figure 12: Wind turbine model in Simulink

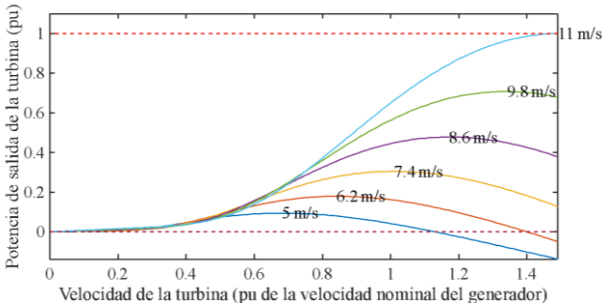

Figure 13: Power output as a function of wind speed

From [17] it is possible to represent the equations of the wind turbine, in this way the value of the turbine power output according to the variation of the wind speed can be found by equation (9).

$$\boldsymbol{P_m = \frac{1}{2} * C_p(\lambda, \beta) * \rho * A * V^3} \qquad (9)$$

Where $C_p(\lambda,\beta)$, is the coefficient of performance of the turbine, is the density of the air being considered a constant of the system, , is the area of the rotor, , is the wind speed, to obtain the value of equation (10) is used.$\rho, AVC_p(\lambda,\beta)$

$$C_p(\lambda,\beta) = C_1 * \left(\frac{C_2}{\lambda_i} - C_3 * \beta - C_5\right) * e^{\frac{-C_6}{\lambda_i}} \quad (10)$$

Where, , is the angle of blade inclination, , is the ratio of rotor blade tip speed to wind speed, , , , and are system constants. To obtain the value of , equation (11) is used.$\beta\lambda C_1C_2C_3C_5C_6\lambda_i$

$$\frac{1}{\lambda_i} = \frac{1}{\lambda + 0.008 * \beta} - \frac{0.035}{1+\beta^3} \quad (11)$$

In addition, to obtain the value of the wind turbine, the mechanical torque and the angular velocity, equations (12), (13) and (14) are used as appropriate.λTw_m

$$\lambda = \frac{w_m * R}{V} \quad (12)$$

$$T = \frac{P_m}{w_m} \quad (13)$$

$$w_m = \frac{\lambda * V}{R} \quad (14)$$

Where , is the rotational speed, , is the radius of the turbine, , is the power output of the turbine, and , is the angular velocity of the turbine.$w_m RP_m w_m$

At the same time, other elements are required to support the hybrid system such as the electric generator, which has the function of taking advantage of the power and torque produced by the wind turbine and therefore producing electrical power, this element is coupled to the output of the wind turbine, and has cylindrical rotor type poles. obtaining a nominal power of . Likewise, a three-phase AC/DC converter connected to the electric generator is considered, as shown in Fig. 14, which is made up of six diodes which have the function of performing the AC/DC conversion, in addition to a capacitor and resistor that perform the filtration of the signal, it should be noted that this conversion process is carried out to connect the wind turbine to the batteries since they work with DC voltage. $43300\ W$

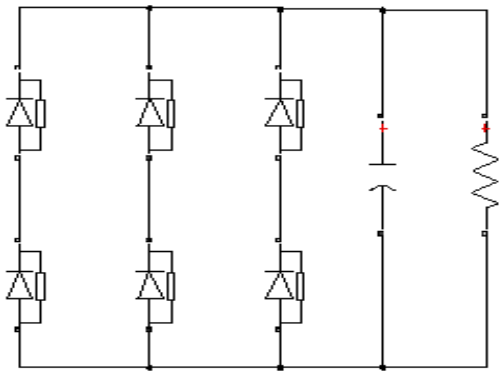

Figure 14: AC/DC converter model

With respect to the storage system, a lithium-ion battery is considered which is connected to the output of the photovoltaic panels and the wind turbine in order to be charged by NCRE, it must be considered that the battery is of and has a capacity of . Depending on the characteristics of the battery, it must be taken into account that all the transformation elements such as the inverter and the converter must be of to guarantee a correct operation of the project. $\mathbf{12\ VDC100\ Ah12\ VDC}$

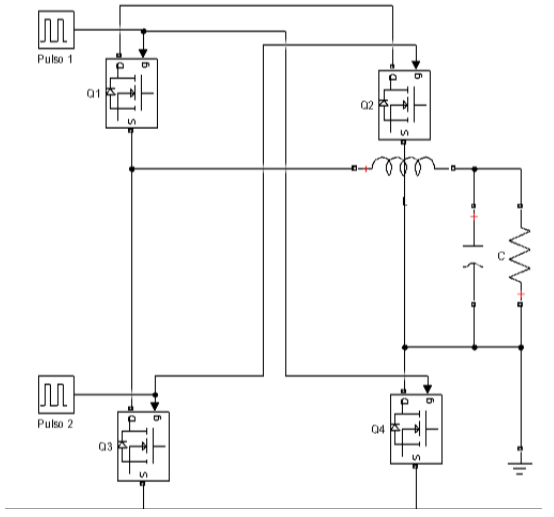

Figure 15: DC/AC Inverter Model

In the system, a DC/AC inverter is considered, which is connected to the storage system, which has the ability to convert the direct voltage to alternating voltage necessary for the load to operate. The inverter model is presented in Fig. 15, which is made up of a bank of 4 mosfets and an RLC filter to obtain a pure sinusoidal signal of both voltage and current, it also has a transformer of $\mathbf{400\ W}$ nominal power, a voltage on the primary side and on the secondary side, characteristics necessary to ensure the supply of cargo.$\mathbf{12\ VDC120\ VAC}$

3. Analysis of Results

In order to observe the output of the simulation of the hybrid system towards the load, an oscilloscope has been located that allows determining the voltage, current and power of the system. In Fig. 16, the graph of the output voltage of the inverter is represented, which shows a pure sine wave of a, which allows defining that these parameters are adequate for the correct operation of the electronic devices that can be supplied by the system.$\mathbf{120}\,\boldsymbol{VAC}\mathbf{60}\,\boldsymbol{Hz}$

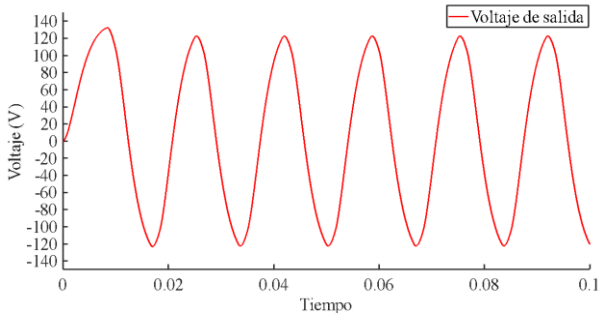

Figure 16: Hybrid System Output Voltage

Similarly, in Fig.17, the graph of the output current of the hybrid system is shown, which is observed as a sinusoidal signal suitable for the operation of the load connected to the inverter output, with a value of $\mathbf{.3,13}\,\boldsymbol{A}$

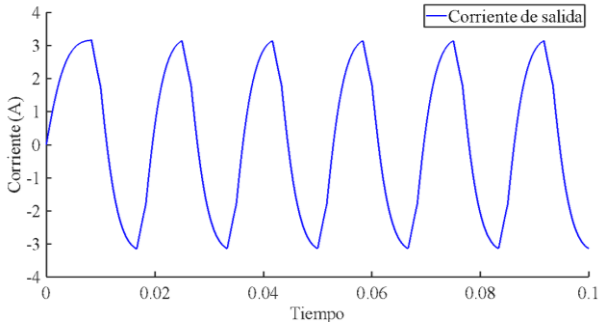

Figure 17: Hybrid system output current

Also in Fig. 18, the power output of the hybrid system is shown, which has a value of , which is sufficient for the adequate supply of the load proposed in the project.$\mathbf{378}\,\boldsymbol{W}$

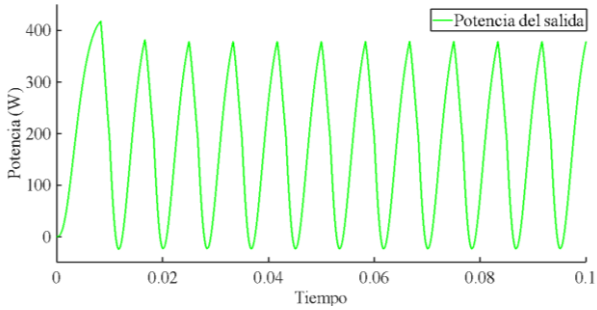

Figure 18: Hybrid system power output

On the other hand, Table 6 presents an analysis of the percentage of battery charge based on the amount of solar and wind resource as input to the hybrid system. Where you can see that the battery is charged at the time of solar radiation and wind speed, to reach the charging it needs a solar radiation of and a wind speed of . Therefore, it is observed that the battery achieves its maximum charge with solar radiation and wind speed, in this way it can be verified that the greater the solar and wind resource the battery will reach, the greater the charge.20 %86,4 $W/m^2$0,9 m/s50 %216 $W/m^2$2,25 m/s432 $W/m^2$4,51 m/s

Table 6: Battery Charge Based on Available Resource

Battery Charge (%)	Solar radiation (W/m^2)	Wind speed (m/s)
0	0	0
20	86,4	0,9
50	216	2,25
70	302,4	3,15
100	432	4,51

Finally, Table 7 shows the effect of battery discharge as a function of the system's output parameters, having voltage, current, and power as a response. It was determined that when charging the battery, the demand is supplied with an output voltage of , for an established power of the load is covered with power and current. In this way, the proper functioning of the battery can be checked in the direction of supplying the demand to the different electronic devices.100 %120 VAC200 W378 W3,13 A

Table 7: Battery discharge for different scenarios

Battery Charge (%)	Voltage (V)	Stream (A)	Power (W)
100	120,5	3,13	378,3
70	111,4	2,90	324
50	111	2,89	321,4
20	108,9	2,83	309,4
0	13,52	0,60	12,58

4. Conclusions and Recommendations

From the analysis of the energy potential that the hybrid system can establish in the San José neighborhood, it is possible to define that the project is feasible to carry out in the established place, since by making real measurements for a month of the resource, maximum

values of solar radiation and wind speed have been obtained. In addition, after extrapolating the data for the entire year 2024 using the Monte Carlo Method, it is possible to identify that the monthly average of the resource in the place corresponds to solar radiation and wind speed, sufficient values to continue with the design and simulation of the project.620 W/m^2 6,49 m/s432 W/m^2 4,51 m/s

The design of the hybrid system was carried out from the lifting of loads, where a maximum demand of with a utilization factor of what represents a power of . From this load, it was possible to determine the technical characteristics that each element of the system must have, both in the solar and wind energy generation stage, as well as in the conversion and investment of energy, and finally in the storage of hybrid energy through batteries to supply the demand to different electronic devices. 400 W0,5200 W

The simulation of the wind-photovoltaic system through Simulink has shown that the set of proposed elements form an adequate hybrid system. Highlighting that the output conditions of the inverter meet the need to supply a proposed load of , since by entering a solar radiation of and a wind speed of , it is possible to obtain an output voltage of , at a current of and a power of . This allows us to conclude that all the elements that make up the hybrid system satisfactorily comply with an efficient and useful technological proposal for the supply of future loads in rural areas, which can even contribute to the current energy crisis that the country is experiencing. 200 W432 W/m^2 4,51 m/s120,5 VAC3,13 A378,3 W

Finally, this document serves as a guide for the practical implementation of the hybrid system, and allows identifying the help provided by academia to communities isolated from the electricity grid, especially in rural areas of Ecuador.

Possible future work could be established based on the improvement of the prototype, both in its design and in its dimensioning, as well as to maximize the supply of the load, improve the technology of the elements, and carry out an implementation that includes different operational tests, which will allow the results of the project to be evidenced in the territory in the near future.

References

[1] Antonio del Rio and Nicté Luna, "Renewable Energies Towards Sustainability," National Autonomous University of Mexico (UNAM), vol. 0.

[2] Galdiano Hernández Marta, "Harnessing Renewable Energies," ICB Publishing House, vol. 2, 2016.

[3] Cáceres César, "Modeling of a hybrid wind-solar system for the analysis of electrification behavior in populations of the Gulf of Guayaquil using Matlab & Simulink," UNIVERSIDAD CATÓLICA DE SANTIAGO DE GUAYAQUIL, Guayaquil, 2024.

[4] Herrera Barros Vanessa Catalina, "Hybrid wind-photovoltaic system for the generation of electricity in the department of tourism of the illustrious municipality of Baños de Agua Santa," Technical University of Ambato, Ambato, 2011.

[5] De Lerma, "Renewable energies as an opportunity and challenge for territorial development, Valle de Lerma, Salta, Argentina," Valle de Lerma. [Online]. Available: http://revistas.unlp.edu.ar/index.php/domus/issue/current/showToc

[6] P. Behera and M. Pattnaik, "Design and real-time implementation of wind–photovoltaic driven

low voltage direct current microgrid integrated with hybrid energy storage system," J Power Sources, vol. 595, Mar. 2024, doi: 10.1016/j.jpowsour.2023.234028.

[7] Gabriel Inca, Daniel Cabrera, Dalton Villalta, Rodrigo Bautista, and Hernan Cabrera, "Evaluation of the current situation of photovoltaic systems in Ecuador: advances, challenges, and perspectives," 20 June 2023.

[8] A. Brizuela, "Non-conventional energy -solar and wind- for rural schools in the province of Entre Ríos," Science, Teaching and Technology Network, 2005.

[9] A. Vera-Dávila, J. Delgado-Ariza, and S. Sepúlveda-Mora, "Validation of the mathematical model of a solar panel using the Matlab Simulink tool," Journal of Research, Development and Innovation, vol. 8, no. 2, pp. 343–356, Jun. 2018, doi: 10.19053/20278306.v8.n2.2018.7972.

[10] D. L. Jiménez, J. Toapanta, P. Muñoz, and R. Salazar, "State-of-Health Assessment of Lithium-Ion Batteries in Two Scenarios: Microgrids and Electric Vehicles," in ECTM 2023 - 2023 IEEE 7th Ecuador Technical Chapters Meeting, Institute of Electrical and Electronics Engineers Inc., 2023. doi: 10.1109/ETCM58927.2023.10309053.

[11] "SILICON-CELL PYRANOMETER METERS | MP-100 & MP-200." [Online]. Available: www.apogeeinstruments.com

[12] Acurite.com. [Online]. Available: https://www.acurite.com/media/manuals/01528-instructions.pdf.

[13] "ECUADORIAN CONSTRUCTION STANDARD NEC-11 CHAPTER 14 RENEWABLE ENERGIES."

[14] "SALESIAN POLYTECHNIC UNIVERSITY GUAYAQUIL HEADQUARTERS ELECTRICITY CAREER ELECTRICAL DESIGN OF A PHOTOVOLTAIC SYSTEM ON GRID FOR THE COMPLEX OF AWARENESS AND CARE OF THE SEA, YUBARTA."

[15] A. G. Vera-Dávila, J. C. Delgado-Ariza, and S. B. Sepúlveda-Mora, "Validation of the mathematical model of a solar panel using Matlab's Simulink tool," Journal of Research, Development and Innovation, vol. 8, no. 2, pp. 343–356, Jun. 2018, doi: 10.19053/20278306.v8.n2.2018.7972.

[16] A. Rocío, E. Rojas Hernández, and E. Díez Fernández, "Spectral characterization of commercial solar cells," 2011.

[17] Mathworks.com, "Implement model of variable pitch wind turbine - Simulink - MathWorks América Latina."